

Syntheses, characterizations, and catalytic activities of mesostructured aluminophosphates with tailorable acidity assembled with various preformed zeolite nanoclusters

Hongri Suo · Shangjing Zeng · Runwei Wang · Zongtao Zhang · Shilun Qiu

Published online: 25 February 2015
© Springer Science+Business Media New York 2015

Abstract A series of ordered hexagonal mesoporous zeolites have been successfully synthesized by the assembly of various preformed aluminosilicates zeolite (MFI, FAU, BEA etc.) with surfactants (cetyltrimethylammonium chloride) under hydrothermal conditions. These unique samples were further characterized by X-ray diffraction, transmission electron microscopy, N₂ adsorption, infrared spectroscopy. Characterization results showed that these samples contain primary and secondary structural building units of various zeolites, which may be responsible for their distinguished acidic strength, suggesting that the acidic strength of these mesoporous silicoaluminophosphates could be tailored and controlled. Furthermore, the prepared samples were catalytically active in the cracking of cumene.

Keywords Mesoporous materials · Heteroatom-substituted AIPOs · Zeolite nanoclusters · Acid strength

1 Introduction

Ever since Mobil corporation reported the first successful preparation of mesoporous materials MCM41S, expanding the variety of such materials for improved stability and desirable physicochemical properties have become an

important research area [1–12]. To this end, the mesoporous materials are either synthesized directly from non-siliceous materials or by introducing a non-siliceous element into meso-silicates, and their potential application as acid or redox catalysts in bulk compound reactions are being continuously explored [13–30]. Zhao et al. [13] reported the synthesis of mesoporous AIPOs using cationic surfactants of cetyltrimethylammonium; Lu et al. investigated the synthesis parameters on the formation of mesoporous [28]; Inagaki et al. prepared stable mesoporous TiAPO with high cation exchange capacity [30]. Although a series of novel mesoporous AIPOs, SAPOs and MAPOs have been successfully synthesized, as mentioned above [12–30], mesoporous aluminosilicophosphates and aluminosilicophosphates have still gained much lesser attention than the aluminosilicates. Only a handful of work has been devoted to-date in the study of synthesis, properties, and potential uses of such materials. One possible reason is probably because a stable structure is difficult to obtain and the pore structure become less ordered after the organic template is removed from the mesoporous materials. However, the possible diverse pore structure and the potential applications in catalysis and sorption have attracted researchers to explore more versatile synthetic strategies to obtain mesoporous aluminophosphates and aluminosilicophosphates with ordered pore structure, thermal stability and catalytic properties. One such strategy involved the use of an assembly of preformed nanosized zeolite precursors with surfactants to form aluminosilicates materials [31–39].

For examples, Xiao et al. have prepared a series of mesoporous materials of MAS-3 [31], MAS-5 [32, 33], MAS-7 [34], MAS-8 [31], MAS-9 [35] and MTS-9 [34, 36, 37] assembled from preformed zeolite of L, β , ZSM-5, and TS-1 nanoclusters in both strongly acidic media and

Electronic supplementary material The online version of this article (doi:10.1007/s10934-015-9923-y) contains supplementary material, which is available to authorized users.

H. Suo · S. Zeng · R. Wang (✉) · Z. Zhang · S. Qiu
State Key Laboratory of Inorganic Synthesis and Preparative and Chemistry, Department of Chemistry, Jilin University, Changchun 130012, People's Republic of China
e-mail: rwwang@jlu.edu.cn; rwwang@mail.jlu.edu.cn

alkaline conditions. Pinnavaia et al. reported the synthesis of Al-MSU-S assembled from zeolite of Y, β , and ZSM-5 seeds solution [38–40]. All of these mesoporous materials showed high hydrothermal stability and good activity in catalytic conversion of organic compounds compared to the conventional mesoporous materials, such as MCM-41 and SBA-15.

Recently, we have successfully prepared mesoporous SAPOs by assembly of zeolite Al-ZSM-5 nanoclusters (denoted as Al-JQW-5) with quaternary alkylammonium surfactants in alkaline media [41]. Here, we show the preparation of various SAPOs by assembly of different aluminosilicates (e.g. MFI, FAU, Bea and LTL) nanoclusters (denoted as Al-JQW-n), and compare the differences in acidities in these samples.

2 Experimental section

2.1 Materials

Fumed silica and sodium silicate (25 % SiO₂, 8 % Na₂O) were purchased from Shenyang Chemical Co. Tetramethylammonium hydroxide (TMAOH), tetraethylammonium hydroxide (TEAOH) and tetrapropylammonium hydroxide (TPAOH) were purchased from Sinopec (China). Phosphoric acid, aluminum iso-propoxide, sodium aluminate, sodium hydroxide, potassium hydroxide, tetraethyl orthosilicate (TEOS), cetyltrimethylammonium chloride (CTAC), ethanol, hydrochloric acid, NH₃·H₂O, NH₄NO₃, sodium silicate, and cumene were purchased from Beijing Chemical Co.

2.2 Syntheses

Al-JQW-5, Al-JQW-6, Al-JQW-7 and Al-JQW-8 were prepared from the assemblies of zeolite ZSM-5, Beta, Y and L nanoclusters, respectively.

The zeolite MFI nanoclusters were prepared by modification of the previously reported method follows [34]: to a mixture of 4 mmol of NaOH, 2.6 mmol of NaAlO₂ and 80 mmol of fumed silica was added 25 mL of TPAOH aqueous solution (20 %) under stirring. The mixture was then transferred into an autoclave and aged for 4 h at 140 °C.

The zeolite beta nanoclusters were prepared by modification of earlier reported methods [34, 36, 37]: to a mixture of 0.16 g of NaOH, 0.30 g of NaAlO₂, and 4.8 g of fumed silica was added 25 mL of TEAOH aqueous solution (20 %) under stirring. The mixture was then transferred into an autoclave for aging for 4 h at 140 °C to obtain a clear solution.

With a slight modification of an earlier method [36], the zeolite Y nanoclusters were prepared. To a solution of

1.6 g NaOH and 0.5 g NaAlO₂ in 5 mL of H₂O, 10.9 g of sodium silicate (Na₂O/SiO₂/H₂O = 1/4.6/30.5) was added. The mixture was left for aging at room temperature for 48 h.

To prepare zeolite L nanoclusters by modification of an earlier method [31], 23 mmol of NaOH, 4.8 mmol of KOH and 2.7 mmol of NaAlO₂ were first dissolved in 3.6 mol of H₂O. Then 13.8 mL of sodium silicate (Al₂O₃/SiO₂/Na₂O/K₂O/H₂O molar ratio of 1/60/7.2/10.8/540) was added to this solution under stirring, followed by aging at room temperature for 72 h.

In typical synthesis: (1) 12 mmol of aluminum isopropoxide was slowly added into 14.4 ml water containing 18 mmol of phosphoric acid (85 %) under vigorous stirring; (2) 5 mmol of CTAC was dissolved in H₂O (2.7 mol) under stirring and followed by adding the aluminophosphate gel; (3) 1.8 ml of preformed zeolite nanoclusters was added into the above mixture, and then TMAOH aqueous solution (20 %) was added drop wise until the pH of the mixture was 9.0; (4) the obtained mixture was transferred into an autoclave for further condensation at 80 °C for 2 days; (5) the product was filtered, washed by water for several times, and then dried. Such products were defined as as-synthesized Al-JQW-n (n = 5, 6, 7 and 8); as-synthesized Al-JQW-n was heated at 100 °C for 1 h under N₂, and then calcined at 500 °C for 4 h to remove the surfactants of CTAC and templates of TPAOH, the samples had not any organic templates, which were defined as calcined Al-JQW-n.

For comparison, mesoporous SAPO was also synthesized using TEOS as silica source according to a previous procedure [28]. H-formed samples were prepared by ion-exchange with 0.1 M NH₄NO₃ solution at 60 °C, followed by calcination at 550 °C for 2 h.

2.3 Characterizations

The X-ray powder diffraction (XRD) patterns of the samples were obtained with a Siemens D5005 diffractometer using CuK α ($\lambda = 1.54 \text{ \AA}$) radiation. The surface area and pore size of the samples were measured by nitrogen isotherms at $-196 \text{ }^\circ\text{C}$ using a Micromeritics ASAP 2010 system. The pore-size distribution for the mesoporous samples was calculated using the Barrett–Joyner–Halenda (BJH) model. The sample compositions were determined by inductively coupled plasma (ICP) with a Perkin-Elmer plasma 40 emission spectrometer. Infrared (IR) spectra of the samples were recorded on a Perkin-Elmer FT-IR spectrometer (PE430) with a resolution of 1 cm^{-1} . Temperature-programmed-desorption of ammonia (TPD-NH₃) curves were performed in the range of 120–600 °C at the rate of 15 °C/min. The adsorption of ammonia on the sample was performed at room temperature, followed by

removal of physical adsorption of ammonia at 120 °C for 1 h in pure flowing nitrogen. ^{27}Al , ^{31}P and ^{29}Si NMR spectra were recorded on a Varian Infinity plus 400 spectrometer, fitting the samples in a 7 mm ZrO_2 rotor, spinning at 8 kHz.

2.4 Catalytic test

Catalytic cracking of cumene was performed using the pulse method, and analyses of the catalytic products were carried out with Aglient 6890A gas chromatographs equipped with TCD and FID detectors. The catalytic cracking was performed using the following standard parameters: mass of the catalyst was 0.051 g; reaction temperature was in the range of 250–320 °C (no thermal cracking); the ratio of cumene to the catalyst was 0.4 L/0.050 g. Nitrogen was used as the carrier gas at a flow rate of 0.92 mL/s.

3 Results and discussions

3.1 X-ray diffraction and transmission electron microscopy

The small-angle X-ray diffraction (XRD) patterns and transmission electron microscopy images of various calcined samples are shown in Figs. 1 and 2, respectively. All the samples exhibited three distinct peaks, which can be indexed as (100), (110) and (200) associated with 2-d hexagonal symmetry (Fig. 1) similar to MCM41S. The (100) peaks reflect d spacing at nearly 4 nm, analogous to our previous report [41]. TEM images confirmed the hexagonal arrays of the mesopores with a uniform pore size. From the high contrast in the TEM images of the samples, the distances between mesopores were estimated to be about 4.5 nm, which was consistent with the results of XRD. The wall thickness of the samples was also estimated as 2.0 nm, and pore size was calculated as ~ 2.5 nm.

Notably, no diffraction peak was observed in the region of higher angles 10° – 40° for all Al-JQW-n samples (supporting Figure 1), which indicated the absence of large microporous crystals in the sample, suggesting that Al-JQW-n samples comprised of pure phase and were not zeolites in nature.

3.2 Nitrogen adsorption isotherms

Figure 3 shows N_2 adsorption–desorption isotherms for various calcined samples, and the parameters have been summarized in Table 1. Both the N_2 isotherms showed typical IV curves with capillary condensation step at relative pressure (P/P_0) of 0.3–0.4, a typical characteristic of

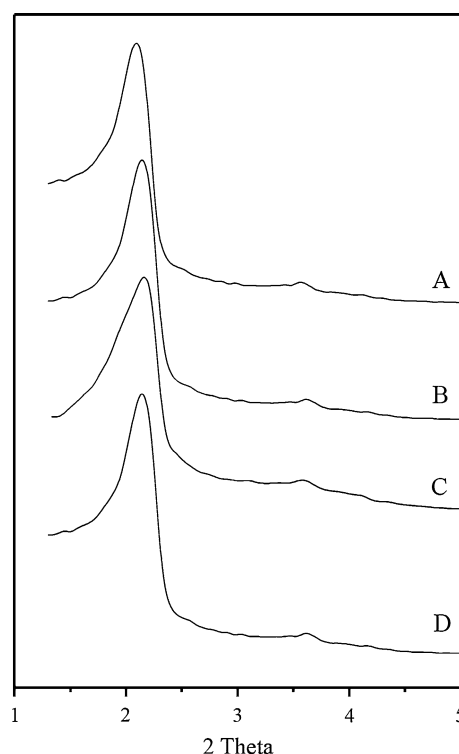


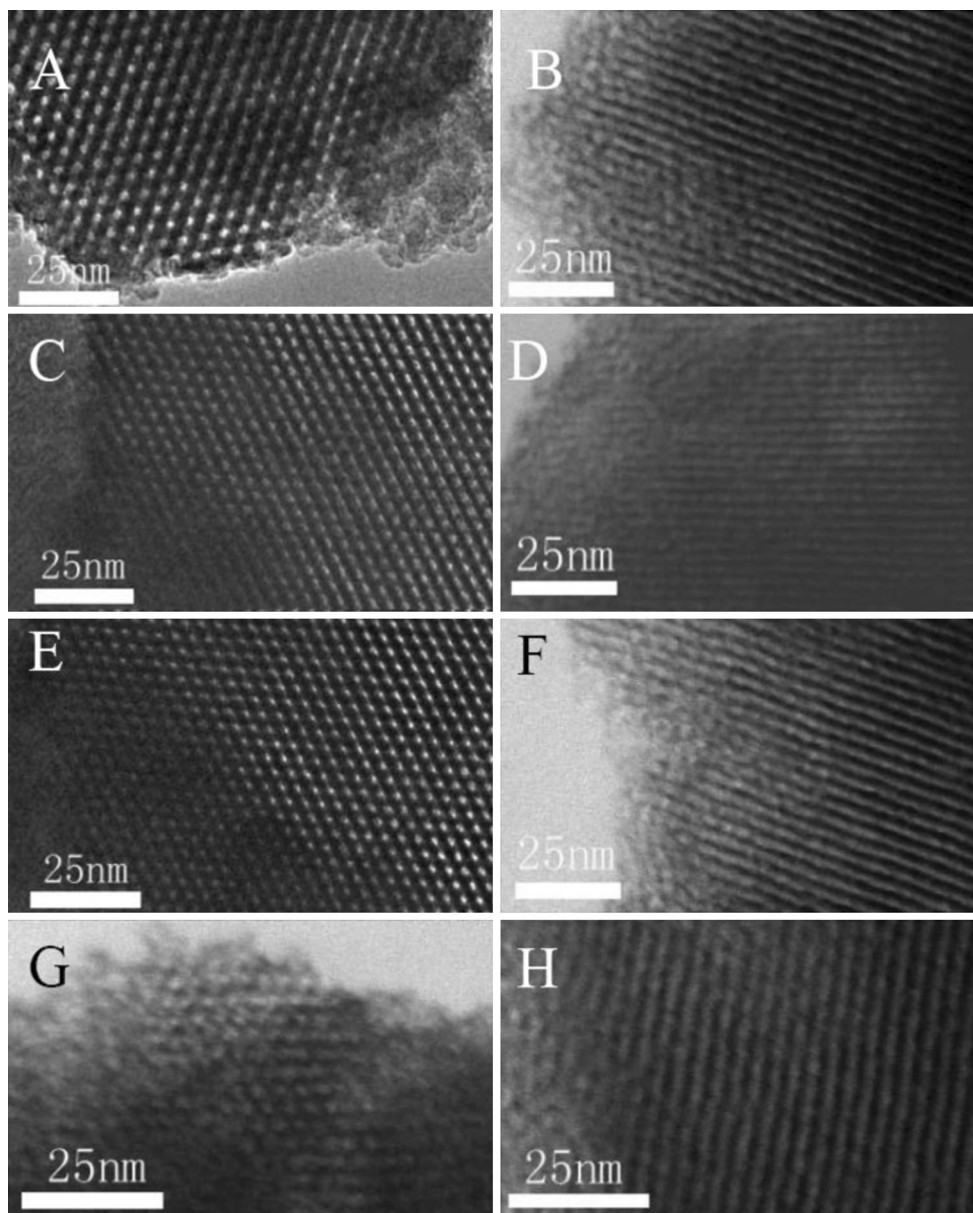
Fig. 1 The small-angle X-ray diffraction patterns of calcined *a* Al-JQW-5, *b* Al-JQW-6, *c* Al-JQW-7, and *d* Al-JQW-8 samples

mesoporous materials. The pore size distribution for all the samples showed a very narrow uniform distribution with a maximum at about 2.5 nm (Fig. 4 inlet), similar to estimated values from the TEM images in Fig. 2. It should be noted that the wall thicknesses of these samples were nearly 2 nm, which was much thicker than that of the conventional mesoporous SAPOs using TEOS as silica source (1.2 nm). This can be reasonably assigned to the existence of preformed zeolite nanoclusters. The zeolite nanoclusters have a larger volume than the silicon species in conventional SAPOs. Therefore, the assembly of these nanoclusters needs more space to connect with each other. It should be noted that most reported mesoporous aluminosilicates or titanosilicates (MAS-7, 8, 9 or MST-9 et al.) prepared via the assembly of preformed zeolite nanoclusters are at least 2 nm thicker than conventional mesoporous materials [34, 37]. In our case, the difference of wall thickness is only 0.8 nm, which is due to much less amount of preformed zeolite nanocluster used in preparation of Al-JQW-5,6,7,8 than that used for MAS series samples.

3.3 Infrared

Figure 4 shows the IR spectra of various samples. Both Al-JQW-5 and Al-JQW-6 showed an obvious band at near 550 cm^{-1} in addition to the broad bands at near 460 cm^{-1} ,

Fig. 2 TEM images of calcined **a** Al-JQW-5, **c** Al-JQW-6, **e** Al-JQW-7, and **g** Al-JQW-8 in [100] direction and **b** Al-JQW-5, **d** Al-JQW-6, **f** Al-JQW-7, and **h** Al-JQW-8 in [110] direction



which were assigned to the amorphous materials [31, 34, 37]. The band at near 550 cm^{-1} was proposed as the characteristic of 5-member rings of T–O–T (T = Si, Al, Ti) in MFI and BEA zeolites in earlier reports [34, 37, 42, 43]. The Al-JQW-7 sample showed the obvious band at 580 cm^{-1} , assigned to the D6R in Y zeolite. The Al-JQW-8 sample displayed distinguishable bands at near 600, 480, and 440 cm^{-1} , which were very similar to those in zeolite L and mesoporous aluminosilicates (MAS-3 and MAS-8) assembled from preformed zeolite L precursors [31], indicating that the mesoporous walls of Al-JQW-8 contained primary and secondary building units of zeolite L [31]. The above results confirmed that nanoclusters

containing zeolite primary and secondary building units had been incorporated into the walls of mesoporous SAPOs.

3.4 NMR studies

3.4.1 ^{27}Al MAS NMR

^{27}Al MAS NMR spectra of all the samples before and after calcinations are shown in Fig. 5. Before calcination, all the samples exhibited one strong peak at 50 ppm with an additional weak shoulder at 59 ppm and one weak peak at -1.0 ppm. The peak at 50 ppm can be assigned to

4-coordinated Al (including AlO_4 species bonded to Si_3P and 4P), and the peak at -1 ppm can be attributed to octahedral Al species, which is in accord with previous reports [23, 28]. The chemical shifts at 57–59 ppm among SAPOs materials had also been observed in our previous report on assemble with TS-1 and MFI nanoclusters. [41]. These results suggested that the environment of partial aluminum atoms in all the samples was much similar to that in zeolites.

In comparison to the as-synthesized samples, all the peaks shifted to lower frequencies after calcinations (Fig. 5d–f). The as-calcined samples exhibited strong peaks in the range of 44–46 and weak peaks at (-3) to (-5) ppm attributed to 4- and 6-coordinated Al species, respectively [22–24, 28]. The shoulder shifted to

54–56 ppm, suggesting that those aluminum atoms were similar to zeolite and existed after calcinations.

3.4.2 ^{31}P MAS NMR

^{31}P MAS NMR spectra of all the samples before and after calcinations are presented in Fig. 6. Only one peak was observed for all the samples both before and after calcinations, indicating a uniform environment of the phosphate atoms. It has been reported that chemical shifts of ^{31}P of aluminophosphates fall in the range -19 to -30 ppm, and were assigned to tetrahedral phosphate species [14, 22–24]. As observed in Fig. 6, peak at nearly -19 (before calcinations) and -28 ppm (after calcinations) can be attributed

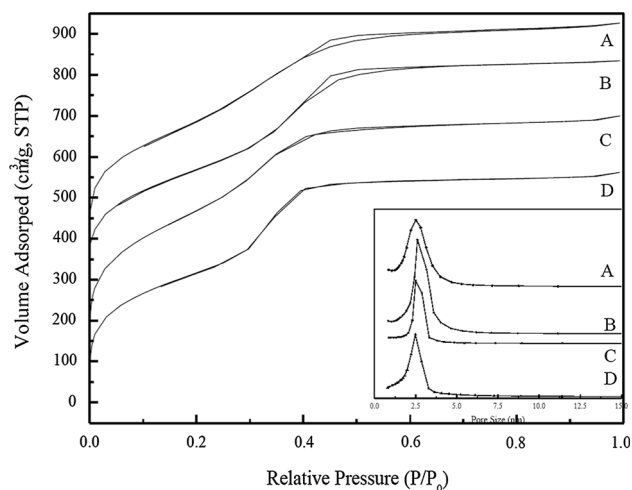


Fig. 3 N_2 adsorption/desorption isotherms for calcined *a* Al-JQW-5, *b* Al-JQW-6, *c* Al-JQW-7, and *d* Al-JQW-8 samples. *Inset* Pore size distribution for calcined *a* Al-JQW-5, *b* Al-JQW-6, *c* Al-JQW-7, and *d* Al-JQW-8 samples

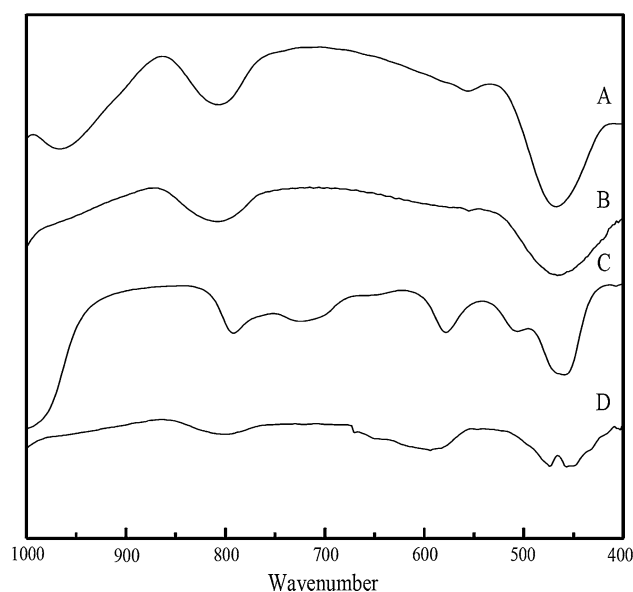


Fig. 4 IR spectra of calcined *a* Al-JQW-5, *b* Al-JQW-6, *c* Al-JQW-7, and *d* Al-JQW-8 samples

Table 1 Physical parameters and catalytic conversions of cracking cumene over various samples

Samples	Molar ratio of products		Pore size (nm)	Wall thickness (nm)	Surface area (m^2/g)	Pore volume (cm^3/g)	Cumene conversion (%)
	Si/Al	P/Al					
Al-JQW-5	0.33	0.74	2.48	2.05	927	0.59	43.2
Al-JQW-6	0.36	0.74	2.56	1.97	891	0.58	42.8
Al-JQW-7	0.34	0.73	2.39	1.96	868	0.57	35.7
Al-JQW-8	0.35	0.74	2.36	1.98	901	0.58	32.3
SAPO	0.35	0.73	2.35	1.24	1007	0.65	29.1

The molar ratio of products were detected by ICP

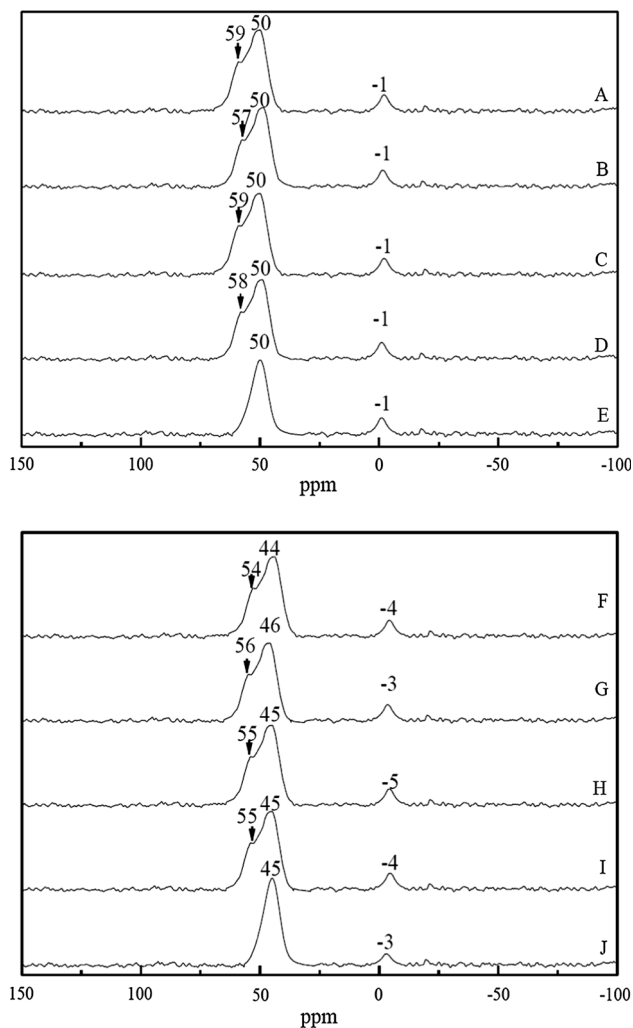


Fig. 5 ^{27}Al MAS NMR spectra for as-synthesized samples of *a* Al-JQW-5, *b* Al-JQW-6, *c* Al-JQW-7, *d* Al-JQW-8, *e* SAPOs and calcined samples of *f* Al-JQW-5, *g* Al-JQW-6, *h* Al-JQW-7, *i* Al-JQW-8 and *j* SAPOs

to tetrahedral phosphate according to the previous report [28].

3.4.3 ^{29}Si MAS NMR

^{29}Si MAS NMR spectra of calcined samples are shown in Fig. 7. All the samples displayed a broad peak at nearly -92 ppm, which may be attributed to all the Si sites of Si(4Al), Si(3Al) and Si(2Al) totally ($Q^2 + Q^1 + Q^0$). Additionally, the spectra of all the samples exhibited two strong peaks at -101 and -110 ppm, assigned to Si(1Al) (Q^3) and Si(4Si) (Q^4), respectively [28, 44, 46, 47].

As shown in Fig. 7, the intensity of the peak at -92 ppm in the spectrum of SAPOs was much higher than those of Al-JQW samples, suggesting that the number of Si sites of ($Q^2 + Q^1 + Q^0$) in conventional mesoporous

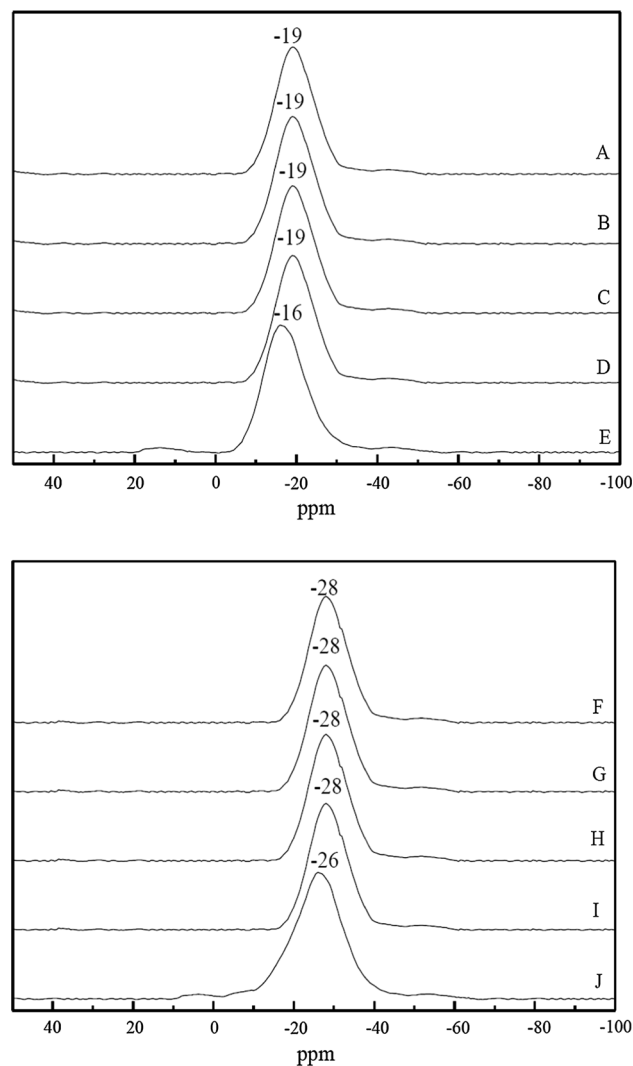


Fig. 6 ^{31}P MAS NMR spectra for as-synthesized samples of *a* Al-JQW-5, *b* Al-JQW-6, *c* Al-JQW-7, *d* Al-JQW-8, *e* SAPOs and calcined samples of *f* Al-JQW-5, *g* Al-JQW-6, *h* Al-JQW-7, *i* Al-JQW-8 and *j* SAPOs

SAPOs are larger than those in Al-JQW-*n* samples. On the contrary, the intensity of the peak at -110 ppm in the spectrum of SAPOs is lower than those of Al-JQW samples, indicating there are more Si(4Si) sites (Q^4) in Al-JQW samples rather than in conventional mesoporous SAPOs. These results can be explained by the fact that Al-JQW-5 and Ti-JQW-5 samples contain zeolite nanoclusters, in which most of the Si atoms are Q^4 and Q^3 analogue of zeolites [34, 35]. Similar phenomenon has also been reported in our previous report [41, 45].

3.5 Acidity

Temperature programmed desorption of ammonia (TPD- NH_3) curves for Al-JQW-*n* and conventional mesoporous

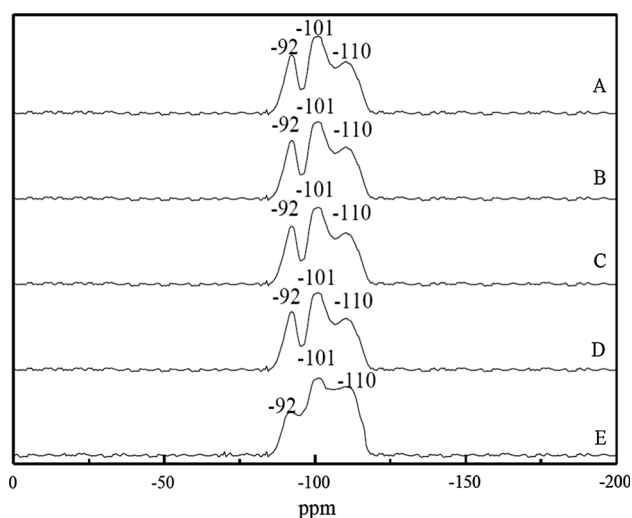


Fig. 7 ^{29}Si MAS NMR spectra for calcined samples of *a* Al-JQW-5, *b* Al-JQW-6, *c* Al-JQW-7, *d* Al-JQW-8, *e* SAPOs

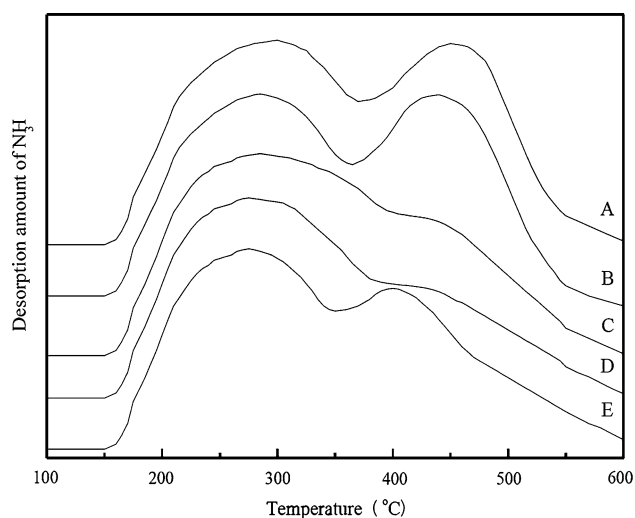


Fig. 8 NH_3 -TPD curves of *a* Al-JQW-5, *b* Al-JQW-6, *c* Al-JQW-7, *d* Al-JQW-8, *e* SAPOs samples

SAPOs, prepared using TEOS as silica source, have been shown in Fig. 8. All samples showed one desorption peak in the range of 260–320 °C as weak or mild acid sites and another desorption peak in the range of 400–460 °C as strong acid sites. Al-JQW-5 prepared from the assembly of zeolite MFI nanoclusters displayed two peaks at 300 and 450 °C, Al-JQW-6 prepared from the assembly of zeolite BEA nanoclusters showed two peaks at 285 and 440 °C, Al-JQW-7 prepared from the assembly of zeolite Y nanoclusters presented a broad peak at 280 °C with a shoulder peak at 435 °C, and Al-JQW-8 prepared from the assembly of zeolite L nanoclusters produced one broad peak at 275 °C as well as a shoulder peak at 430 °C. On the other hand, conventional mesoporous SAPOs showed two peaks

at 275 and 400 °C, indicating that the acidity of Al-JQW samples were higher than the conventional mesoporous SAPOs.

The acidity of aluminum-containing catalyst is often influenced by the local environment of Al atoms. As discussed above, ^{27}Al MAS NMR spectrum of Al-JQW sample exhibited three peaks including a shoulder peak similar to that of zeolite, suggesting that the environment of partial aluminum atoms is much similar to that of zeolite rather than that incorporated within the amorphous walls of the conventional mesostructured materials. Such local environment of Al atoms may be responsible for the stronger acidity than SAPOs. Furthermore, acidities of various Al-JQW samples assembled from various zeolite precursors were distinguishable. The order of acidic strength was as follows: Al-JQW-5 > Al-JQW-6 > Al-JQW-7 > Al-JQW-8, which signified that the acidities of various zeolite were also distinguishable. As discussed in the previous report [42, 46] that the order of acidic strength for the zeolite was as follows: MFI > BEA > Y > L. Additionally, mesoporous aluminosilicates assembled from various zeolite precursors also showed acidities in the same order [47].

In the catalytic cracking of cumene, all the samples were active, giving the conversion in the range 29.1–43.2 %. The conventional mesoporous SAPOs showed the lowest conversion at 29.1 %, while Al-JQW-5 showed the highest activity, giving the conversion at 43.2 %. The order of conversion was as follows: Al-JQW-5 > Al-JQW-6 > Al-JQW-7 > Al-JQW-8 > SAPOs, confirming the TPD- NH_3 results.

4 Conclusions

To conclude, it can be said that a series of hexagonal mesoporous SAPOs were prepared via the assembly of various aluminosilicates nanoclusters with surfactant, which exhibited different acidity according to the aluminosilicates in the framework. Furthermore, all of the samples displayed catalytic activity in the cracking of cumene.

Acknowledgments This work was supported by National Natural Science Foundation of China (21390394), the National Basic Research Program of China (2012CB821700, 2011CB808703), NSFC (21261130584, 91022030), “111” project (B07016), Award Project of KAUST (CRG-1-2012-LAI-009) and Ministry of Education, Science and Technology Development Center Project (20120061130012).

References

1. S.T. Wilson, B.M. Lok, C.A. Messina, T.R. Cannan, E.M. Flanigen, *J. Am. Chem. Soc.* **104**, 1146 (1982)
2. B.M. Lok, C.A. Messina, R.L. Patton, R.T. Gajek, T.R. Cannan, E.M. Flanigen, *J. Am. Chem. Soc.* **106**, 6092 (1984)

3. E.M. Flanigen, B.M. Lok, R.L. Patton, S.T. Wilson, in *New Developments in Zeolite Science and Technology, Studies in Surface Science and Catalysis*, vol. 28, ed. by Y. Murakami, A. Iijima, J.W. Ward (Elsevier, Amsterdam, 1986), p. 103
4. E.M. Flanigen, R.L. Patton, S.T. Wilson, in *Innovation in Zeolite Materials Science, Studies in Surface Science and Catalysis*, vol. 37, ed. by P.J. Grobet, W.J. Mortier, E.F. Vansant, G. Schulz-Eklo (Elsevier, Amsterdam, 1988), p. 13
5. M. Hartmann, L. Kevan, *Chem. Rev.* **99**, 635 (1999)
6. J.M. Thomas, R. Raja, G. Sankar, R.G. Bell, *Nature* **398**, 227 (1999)
7. R. Raja, G. Sankar, J.M. Thomas, *Angew. Chem. Int. Ed.* **39**, 2313 (2000)
8. M. Dugal, G. Sankar, R. Raja, J.M. Thomas, *Angew. Chem. Int. Ed.* **39**, 2310 (2000)
9. J.D. Chen, R.A. Sheldon, *J. Catal.* **153**, 1 (1995)
10. M.H. Zahedi-Niaki, M.P. Kapoor, S. Keliaguine, *J. Catal.* **177**, 231 (1998)
11. J.S. Beck, J.C. Vautuli, W.J. Roth, M.E. Leonowicz, C.T. Kresge, K.D. Schmitt, C.T.-W. Chu, D.H. Olson, E.W. Sheppard, J.B. Higgins, J.L. Schlenker, *J. Am. Chem. Soc.* **114**, 10834 (1992)
12. S. Oliver, A. Kuperman, N. Coombs, A. Lough, G.A. Ozin, *Nature* **378**, 47 (1995)
13. D. Zhao, Z. Luan, L. Kevan, *Chem. Commun.* 1009 (1997)
14. Z. Luan, D. Zhao, H. He, J. Klinowski, L. Luan, *J. Phys. Chem. B* **102**, 1250 (1998)
15. Q. Gao, R. Xu, J. Chen, R. Li, S. Li, S. Qiu, Y. Yue, *J. Chem. Soc., Dalton Trans.* 3303 (1996)
16. Q. Gao, J. Chen, R. Xu, Y. Yue, *Chem. Mater.* **9**, 457 (1997)
17. T. Kimura, Y. Sugahara, K. Kuroda, *Chem. Lett.* 983 (1997)
18. T. Kimura, Y. Sugahara, K. Kuroda, *Microporous Mesoporous Mater.* **22**, 115 (1998)
19. T. Kimura, Y. Sugahara, K. Kuroda, *Chem. Commun.* 559 (1998)
20. T. Kimura, Y. Sugahara, K. Kuroda, *Chem. Mater.* **11**, 508 (1999)
21. P. Feng, Y. Xia, J. Feng, X. Bu, G.D. Stucky, *Chem. Commun.* 949 (1997)
22. Y.Z. Khimyak, J. Klinowski, *Chem. Mater.* **10**, 2258 (1998)
23. Y.Z. Khimyak, J. Klinowski, *Phys. Chem. Chem. Phys.* **2**, 5275 (2000)
24. Y.Z. Khimyak, J. Klinowski, *Phys. Chem. Chem. Phys.* **3**, 1544 (2001)
25. B. Chakraborty, A.C. Pulikottil, S. Das, B. Viswanathan, *Chem. Commun.* 911 (1997)
26. B.T. Holland, P.K. Isbester, C.F. Blanford, A. Stein, *J. Am. Chem. Soc.* **119**, 6796 (1997)
27. X.S. Zhao, G.Q. Lu, *Microporous Mesoporous Mater.* **44**, 185 (2001)
28. X.S. Zhao, G.Q. Lu, A.K. Whittaker, J. Drennan, H. Xu, *Microporous Mesoporous Mater.* **55**, 51 (2002)
29. E. Gianotti, E.C. Olivera, S. Coluccia, H.O. Pastore, L. Marchese, *Inorg. Chim. Acta* **349**, 259 (2003)
30. A. Bhaumik, S. Inagaki, *J. Am. Chem. Soc.* **123**, 691 (2001)
31. Y. Di, Y. Yu, Y. Sun, X. Yang, S. Lin, M. Zhang, S. Li, F.-S. Xiao, *Microporous Mesoporous Mater.* **62**, 221 (2003)
32. Z. Zhang, Y. Han, L. Zhu, R. Wang, Y. Yu, S. Qiu, D. Zhao, F.-S. Xiao, *Angew. Chem. Int. Ed. Engl.* **40**, 1258 (2001)
33. Z. Zhang, Y. Han, L. Zhu, R. Wang, Y. Yu, S. Qiu, D. Zhao, F.-S. Xiao, *J. Am. Chem. Soc.* **123**, 5014 (2001)
34. Y. Han, F.-S. Xiao, S. Wu, Y. Sun, X. Meng, D. Li, S. Lin, F. Deng, X. Ai, *J. Phys. Chem. B* **105**, 7963 (2001)
35. Y. Han, S. Wu, Y. Sun, D. Li, F.-S. Xiao, J. Liu, X. Zhang, *Chem. Mater.* **14**, 1144 (2002)
36. Y. Liu, W. Zhang, T.J. Pinnavaia, *J. Am. Chem. Soc.* **122**, 8791 (2000)
37. Y. Liu, W. Zhang, T.J. Pinnavaia, *Angew. Chem. Int. Ed.* **40**, 1255 (2001)
38. Y. Liu, T.J. Pinnavaia, *Chem. Mater.* **14**, 3 (2002)
39. K.S.W. Sing, D.H. Everett, R.A.W. Haul, L. Moscou, R.A. Pierotti, J. Rouquerol, T. Siemieniowska, *Pure Appl. Chem.* **57**, 603 (1985)
40. D.W. Breck, *Zeolite Molecular Sieves* (Wiely, New York, 1974)
41. R. Wang, L. Xu, L. Zhao, B. Chu, L. Hu, C. Shi, G. Zhu, S. Qiu, *Microporous Mesoporous Mater.* **83**, 413 (2005)
42. P.A. Jacobs, E.G. Derouane, J. Weitkamp, *J. Chem. Soc. Chem. Commun.* 591 (1981)
43. E. Lippma, A. Samoson, M. Magi, *J. Am. Chem. Soc.* **108**, 1730 (1986)
44. S.-I. Lee, H. Chon, *J. Chem. Soc., Faraday Trans.* **93**, 1855 (1997)
45. E.M. Flanigen, B.M. Lok, R.L. Patton, S.T. Wilson, *Pure Appl. Chem.* **58**, 1351 (1996)
46. J.M. Thomas, J. Klinowski, *Adv. Catal.* **33**, 199 (1985)
47. A. Corma, *Chem. Rev.* **97**, 2373 (1997)